



## A simple pan-evaporation model for analysis of climate simulations: Evaluation over Australia

Leon D. Rotstayn,<sup>1</sup> Michael L. Roderick,<sup>2</sup> and Graham D. Farquhar<sup>2</sup>

Received 6 June 2006; revised 24 July 2006; accepted 31 July 2006; published 14 September 2006.

[1] We show that a simple model of pan evaporation (“PenPan”) can be used to analyze monthly mean output from a global climate model (GCM). PenPan is based on a modified version of Penman’s potential evapotranspiration equation. Very good agreement is obtained with observed annual pan evaporation for Australian sites when PenPan is forced by surface observations of radiation, wind speed, humidity and air temperature. When PenPan is forced with monthly mean output from the CSIRO GCM, the results are still satisfactory, but pan evaporation is overestimated over southern Australia, primarily due to excessive surface solar radiation simulated by the GCM. The results suggest that PenPan will be a valuable tool for reconciling observed pan-evaporation trends with climate-model simulations.

**Citation:** Rotstayn, L. D., M. L. Roderick, and G. D. Farquhar (2006), A simple pan-evaporation model for analysis of climate simulations: Evaluation over Australia, *Geophys. Res. Lett.*, 33, L17715, doi:10.1029/2006GL027114.

### 1. Introduction

[2] Measurements of pan evaporation have been used for several decades in agricultural science as an estimate of the “evaporative demand” of the atmosphere. Recent interest in pan evaporation has been provoked by an apparent paradox. On the one hand, a warmer climate associated with the anthropogenic greenhouse effect is expected to have a generally more active hydrological cycle [Folland *et al.*, 2001]. On the other hand, widespread decreases of pan evaporation, averaging 2–4 mm per year per year, were observed over several decades up to about 1990 [e.g., Peterson *et al.* 1995]. While most of these observations have been in the Northern Hemisphere, recent analyses of data from Australia [Roderick and Farquhar, 2004] and New Zealand [Roderick and Farquhar, 2005] have shown similar results. The observed reductions in pan evaporation in the Northern Hemisphere are broadly consistent with observed reductions in solar radiation at the Earth’s surface in the period up to 1990 [Stanhill and Cohen, 2001; Roderick and Farquhar, 2002]. Some of this “solar dimming” is simulated by global climate models (GCMs) that include increases in anthropogenic aerosols [Liepert *et al.*, 2004], suggesting that anthropogenic aerosols probably contributed to the reductions in pan evaporation, at least in the Northern

Hemisphere. However, recent 20th Century GCM simulations that include aerosols seem to capture only a part of the observed solar dimming [Nazarenko and Menon, 2005], so it is not clear to what extent anthropogenic aerosols can explain the observed dimming or the observed reductions in pan evaporation. The results from Australia and New Zealand are even more puzzling than those from the Northern Hemisphere, because it seems unlikely that anthropogenic aerosol changes would be large enough in these regions to substantially affect solar radiation. We were motivated by these considerations to develop a simple model of pan evaporation as a tool for analysis of climate-model simulations.

[3] Mechanistic models of evaporation pans comprising multiple water layers have been developed by Jacobs *et al.* [1998] and Molina *et al.* [2006]. Note that the setup of the pans in both of these studies differed from that of the US Class A pan, since either the sides of the pan were insulated [Molina *et al.*, 2006] or the pan was located on the ground [Jacobs *et al.*, 1998]. (Usually, a Class A pan is mounted on a slatted wooden platform, 0.15 meters above the ground.) Both studies concluded that the pan water was well mixed, so a one-dimensional model would be adequate for many purposes. This suggests that it might be feasible to implement a prognostic equation for pan-water temperature in a climate model. A possible complication with this method is that the water-surface (or “skin”) temperature can differ considerably from the mixed water temperature [Thom *et al.*, 1981].

[4] Another approach to the modeling of pan evaporation uses a modified version of the equation of Penman [1948] for potential evapotranspiration [Thom *et al.*, 1981; Linacre, 1994]. Linacre [1994] referred to his simplified Penman equation as a Penpan equation, and obtained excellent agreement between measured and calculated monthly pan evaporation for a number of sites. A possible advantage of this approach (which is based on the mass and energy balance of the pan) is that the water-surface temperature is eliminated during the derivation of Penman’s equation. This approach is also designed to be used over averaging periods of at least 24 hours, and preferably several days, so that heat storage in the pan can be neglected. In this respect it seems compatible with the use of monthly mean forcing data from a climate model.

[5] We have combined aspects of the models of Thom *et al.* [1981] and Linacre [1994] to create a simple pan-evaporation model (PenPan) for analysis of climate-model simulations. We forced PenPan with output from the CSIRO GCM, and with observational data, and compared the modeled pan-evaporation rates in each case with measured pan-evaporation rates. PenPan, the CSIRO GCM and the data are described in Section 2. Results for Australian sites

<sup>1</sup>Marine and Atmospheric Research, Commonwealth Scientific and Industrial Research Organisation, Aspendale, Victoria, Australia.

<sup>2</sup>Cooperative Research Centre for Greenhouse Accounting, Research School of Biological Sciences, Australian National University, Canberra, ACT, Australia.

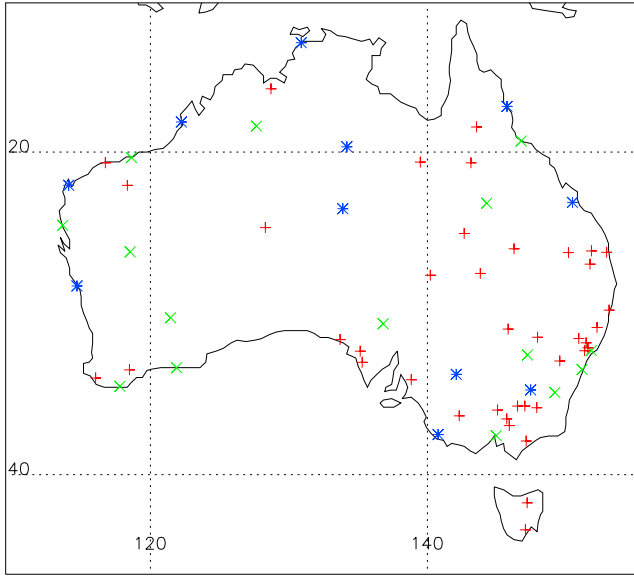


**Figure 1.** Locations of the 70 measurement sites. Blue points show the 11 sites for which pan evaporation can be calculated purely from observations; green points show the other 15 sites for which SW radiation and humidity observations exist; red points show the remaining 46 sites.

and a comparison with measured pan-evaporation rates are presented in Section 3, with conclusions in Section 4. SI units are used for all the equations in Section 2, but the pan-evaporation rates in Section 3 are presented in conventional units (mm per annum or mm per day) for clarity.

## 2. Models and Data

### 2.1. PenPan

[6] Pan evaporation can be modeled using a suitably generalized form of Penman's equation [Thom *et al.*, 1981],

$$LE_p = \frac{s(R_n - S) + L\gamma f_h(u)\delta e}{s + \gamma f_h(u)/f_q(u)}, \quad (1)$$

where  $E_p$  is the pan evaporation rate ( $\text{kg m}^{-2} \text{s}^{-1}$ ),  $L$  is the latent heat of vaporization of water ( $\text{J kg}^{-1}$ ),  $R_n$  is the net irradiance of the pan ( $\text{W m}^{-2}$ ),  $s$  is the slope of the saturation vapor pressure ( $e_s$ ) curve in  $\text{Pa K}^{-1}$ , evaluated at air temperature  $T_a$  (K),  $\delta e = e_s(T_a) - e$  is the vapor pressure deficit (VPD, in Pa),  $\gamma$  is the psychrometric constant ( $\text{Pa K}^{-1}$ ),  $u$  is wind speed at two meters ( $\text{m s}^{-1}$ ), and  $f_h(u)$  and  $f_q(u)$  are the wind functions for transfer of heat and water vapor respectively ( $\text{kg m}^{-2} \text{s}^{-1} \text{Pa}^{-1}$ ). Strictly, Thom *et al.* [1981] required that  $\delta e$  be calculated using the properties of the air just above the surface of the pan (0.41 m above the ground), but they assumed that this was the same as at two meters, except for some hourly calculations at night (when dew was on the ground). We use the properties of the air at two meters, to enable the use of standard GCM output. Further,  $\gamma = c_p p^*/(0.622L)$ , where  $p^*$  is surface pressure and  $c_p$  is the specific heat of dry air at constant pressure, and  $s = Le_s/(R_v T_a^2)$ , where  $R_v$  is the specific gas constant for water vapor.  $S$  is the storage of heat in the pan, which can be neglected for time periods longer than a few days [Thom *et al.*, 1981].

If we define  $a = f_h(u)/f_q(u)$  (the ratio of the effective surface areas for heat and water-vapor transfer), equation 1 can be written as

$$LE_p = \frac{sR_n + La\gamma f_q(u)\delta e}{s + a\gamma}. \quad (2)$$

We use  $a = 2.4$  [Linacre, 1994], larger than the value (2.1) from Thom *et al.* [1981], but smaller than the value (2.5) from Kohler *et al.* [1955]. We use the wind function

$$f_q(u) = 1.39 \times 10^{-8} (1 + 1.35u) \quad (3)$$

derived by Thom *et al.* [1981] using measurements of evaporation from a pan located in a field at the University of Grenoble, France, during the autumn of 1979.

[7] Calculation of  $R_n$  needs to account for the extra shortwave (SW) radiation intercepted by the sides of the pan (including direct, diffuse and reflected radiation). The total SW irradiance of the pan can be estimated as [Linacre, 1994]

$$R_{sp} = [f_{dir}P_{rad} + 1.42(1 - f_{dir}) + 0.42A_s]R_s, \quad (4)$$

where  $R_s$  is the downward solar irradiance at the surface,  $f_{dir}$  is the fraction of  $R_s$  that is direct,  $A_s$  is the albedo of the ground surrounding the pan, and  $P_{rad}$  is the pan radiation factor, which accounts for the extra direct irradiance intercepted by the walls of the pan when the sun is not directly overhead. The factor of 0.42 appears because, for a Class A pan, the water surface area is  $1.15 \text{ m}^2$ , the wall area is  $0.97 \text{ m}^2$ , and the vertical walls are effectively exposed to half of the diffuse and reflected irradiance; then  $0.42 = 0.5 \times 0.97/1.15$  [Linacre, 1994]. The three terms in square brackets thus represent the direct, diffuse and reflected components respectively. The implied increase of SW irradiance relative to that at the ground is substantial; over Australia, the ratio  $R_{sp}/R_s$  ranges from 1.46 in the far north to 1.54 over Tasmania. We set  $A_s = 0.22$ , a value appropriate for short, green grass. In arid regions, the albedo of the bare ground around a pan can be as high as 0.30 [Linacre, 1994], so this is a possible source of error in the model. In annual-mean terms, Linacre [1994] derived  $P_{rad} = 1.32 + 4 \times 10^{-4} \phi + 8 \times 10^{-5} \phi^2$ , where  $\phi$  is the absolute value of latitude in degrees. We adopt  $A_p = 0.14$  as a typical value for the albedo of a Class A pan [Linacre, 1992]. Then

$$R_n = (1 - A_p)R_{sp} + R_l, \quad (5)$$

where  $R_l$  is the net longwave (LW) irradiance of the pan. Note that using an annual-mean expression for  $P_{rad}$  underestimates  $R_{sp}$  for larger solar zenith angles, but this is offset by the use of a fixed albedo for the pan, since in reality the pan's albedo is larger when the sun is lower in the sky. Accurate calculation of  $R_l$  is a complex problem, since it is affected by the geometry of the pan, and the different temperature and emissivity of the water surface relative to the sides of the pan. Linacre [1994] assumed a fixed value of  $-40 \text{ W m}^{-2}$  for the net LW irradiance, but this seems too inflexible for climate-change studies. For

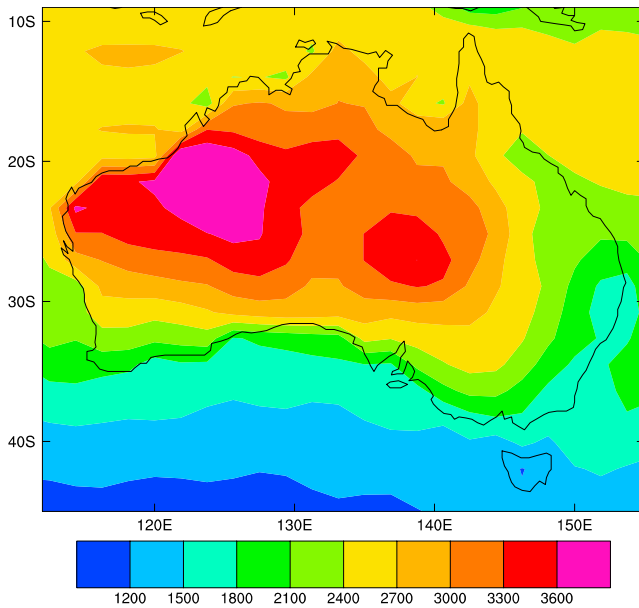


**Figure 2.** Modeled annual pan evaporation (in mm) over Australia, when PenPan is forced by five years of monthly mean output from the CSIRO Mk3 GCM.

simplicity, we assume that the downward component of  $R_l$  at the pan water surface is the same as the downward LW irradiance at the ground, and that the pan water surface radiates as a black body with temperature  $T_a$ . We currently ignore any LW interactions between the air and the sides of the pan. *Linacre* [1994] proposed an additional longwave irradiance from the ground into the sides of the pan in “dry” months, but when we included this correction, PenPan tended to overestimate  $E_p$ . For this reason, and because *Linacre* unrealistically assumed that the pan wall radiates as a black body, we omitted his aridity correction from PenPan.

[8] The evaporation rate given by equation 2 should be reduced when a bird guard is fitted to the pan. For the Class A pan network of the Australian Bureau of Meteorology, this reduction was found empirically to be about 7% [*van Dijk*, 1985], so we multiply equation 2 by 0.93.

## 2.2. Climate Model and Observations

[9] An earlier version of the CSIRO Mk3 Atmospheric GCM was described by *Gordon et al.* [2002]. It has horizontal resolution of spectral T63 (roughly  $1.9^\circ$  by  $1.9^\circ$ ) and 18 vertical levels. Recent improvements to the GCM are described by *Rotstayn et al.* (Have Australian rainfall and cloudiness increased due to the remote effects of Asian anthropogenic aerosols?, submitted to *Journal of Geophysical Research*, 2006). These include treatments of sulfate, carbonaceous, dust, volcanic and sea-salt aerosols, and an updated radiation scheme. After a one-year spinup, we ran the GCM for five years using climatological sea-surface temperatures, and forcing for the year 2000. The fields needed to run PenPan were saved as monthly means, namely air temperature, wind speed and VPD at two meters, surface pressure, and downward LW and SW (total and diffuse) irradiance at the surface. For comparison of GCM-derived output with the point observations described below, we used linear interpolation in space to ensure that the

output from the GCM (and PenPan) had the correct geographic coordinates. Note that GCMs are generally unable to resolve steep topography, which could cause errors if the altitude of the measurement site differs substantially from that of the GCM grid box. Since Australia does not have much steep topography, this is unlikely to cause serious errors in this study, but it may be important if PenPan is applied to GCM output in other regions.

[10] We used an observational data set supplied by the Australian Bureau of Meteorology, comprising monthly pan evaporation measurements at 70 sites for the period 1967–2004. The locations of these sites are shown in Figure 1. We averaged the monthly evaporation data over the 25-year period 1980–2004, to avoid the problem of the introduction of bird guards, since all Australian pans had bird guards fitted by 1978. Evaporation measurements commenced at some sites after 1980, but all sites have at least nine complete years of monthly data. Air temperature and rainfall measurements are available for all 70 sites, but other measurements that are useful for reconciling modeled and observed pan evaporation are available at smaller numbers of sites: downwelling SW irradiance, wind speed and humidity (26 sites) and downwelling LW irradiance (11 sites). The temporal coverage of the radiation data is the most limited, with sites generally having from five to 23 complete years of SW data and five to 10 complete years of LW data. The 11 sites with LW data provide all the inputs needed to force PenPan purely by observations, except that the direct fraction of  $R_s$  must be parameterized. We use  $f_{dir} = -0.11 + 1.31 * R_s / R_{st}$ , where  $R_{st}$  is the downwelling SW irradiance at the top of the atmosphere [*Roderick*, 1999]. Also, in the absence of surface pressure observations, the psychrometric constant (in  $\text{Pa K}^{-1}$ ) is estimated as  $\gamma = 67 - 7.2 \times 10^{-3} z$ , where  $z$  is elevation in meters [*Linacre*, 1994]. In the following figures, we show the 11 “elite” sites as blue points, the remaining 15 sites

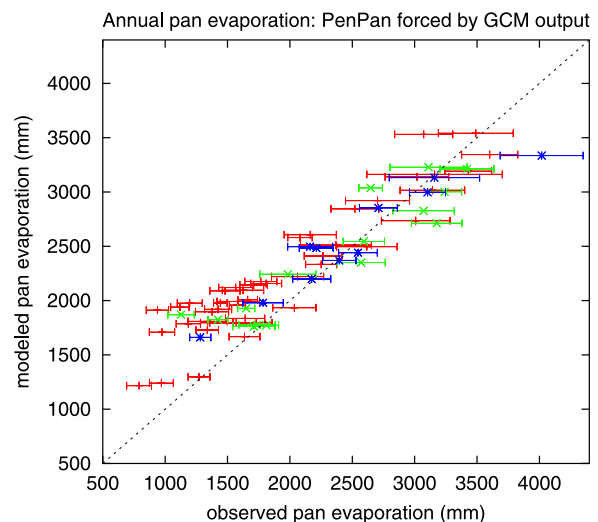


**Figure 3.** Modeled versus observed annual pan evaporation for 70 Australian sites, when PenPan is forced by five years of monthly mean output from the CSIRO Mk3 GCM. Color coding of points is described in the caption of Figure 1. Error bars show  $\pm$  one standard deviation of the annual observations.

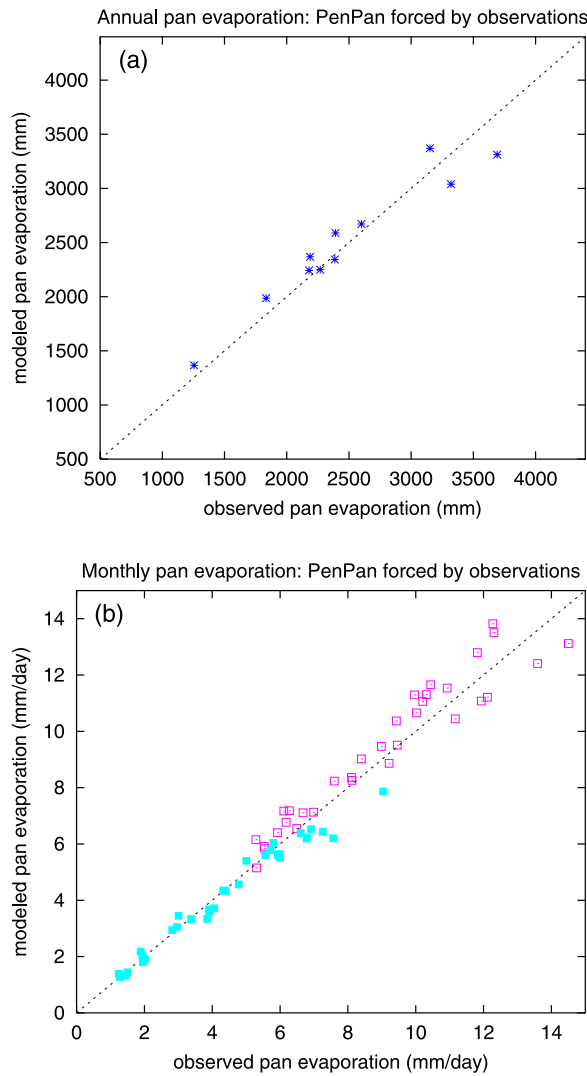


**Figure 4.** Modeled versus observed (a) annual, and (b) monthly mean pan evaporation for 11 Australian sites, when PenPan is forced by observed inputs for individual months. In Figure 4b, solid aqua squares denote winter (June–August) months, and open magenta squares denote summer (December–February) months; data for autumn and spring are omitted for clarity, but similarly follow the 1:1 line.

with SW irradiance, wind speed and humidity measurements as green points, and the other 44 sites as red points.

### 3. Results and Discussion

[11] Figure 2 shows modeled annual  $E_p$  over Australia, when PenPan is forced by output from individual months of the five-year run of the CSIRO Mk3 GCM. The spatial pattern shows smaller values in the south, and larger values in the northwest and central parts of the continent. The modeled values are in reasonable agreement with observations shown for 30 sites in Table A.1 of *Roderick and Farquhar* [2004]. A scatter plot for the 70 sites in our data set (Figure 3) shows that the model is broadly successful at capturing the spatial gradient in  $E_p$ , but tends to overestimate  $E_p$  for smaller values of  $E_p$ .

[12] Is the bias in Figure 3 due to PenPan, the GCM or a combination of both? To resolve this question, we reran PenPan using observed inputs from individual months at the 11 elite sites, and then averaged the data for these months to generate climatological observed and modeled monthly mean  $E_p$ . These climatological observed and modeled monthly mean values were then averaged to obtain annual  $E_p$ , as shown in Figure 4a. Figure 4 shows that generally good results are obtained for both annual and monthly mean  $E_p$ , and that PenPan performs similarly well in the summer and winter seasons. In Figure 3, some of the sites for which PenPan (forced by the GCM) overestimates low values of  $E_p$  are blue points, for which better agreement is seen in Figure 4a. Overall, Figure 4 suggests that the main cause of the overestimated  $E_p$  over southern Australia is one or more of the forcing fields from the GCM.

[13] Both shortwave irradiance ( $R_s$ ) and VPD are expected to have spatial variations similar to those shown for  $E_p$  in Figure 2, and both could contribute to the overestimated  $E_p$  over southern Australia. (We also looked at

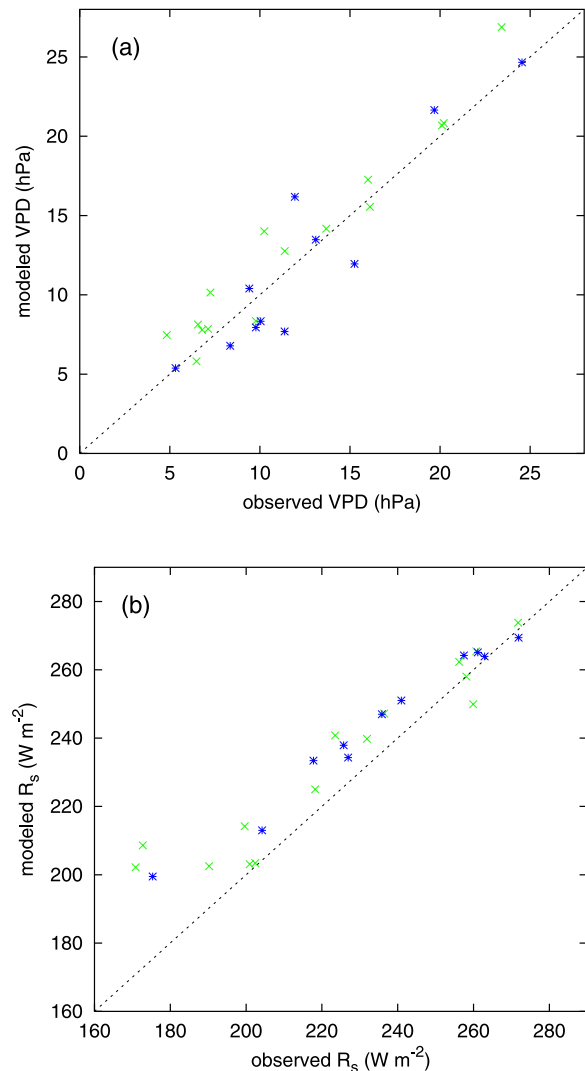


**Figure 5.** GCM-simulated versus observed annual-mean (a) vapor-pressure deficit, and (b) downward solar irradiance at the surface, for 26 Australian sites.

wind speed, but neither the actual wind speed or its bias in the GCM show a coherent spatial pattern in annual-mean terms.) Figure 5 shows annual-mean GCM-simulated versus observed VPD and  $R_s$  at 26 sites for which these data were available. VPD shows no appreciable bias, but  $R_s$  in the GCM shows a substantial overestimate at lower values. The three strongly biased points in the lower left corner of Figure 5b are Mount Gambier (blue point), Albany and Melbourne (green points), and these are also the three most southerly points for which  $R_s$  observations are available. These three points are also seen in Figure 3 as the green and blue points with observed annual  $E_p < 1500$  mm, and indicate that excessive  $R_s$  from the GCM is the primary cause of the overestimated  $E_p$  in the temperate zone. For Mount Gambier, the overestimate of  $R_s$  is  $24 \text{ W m}^{-2}$ , which implies an increase in  $E_p$  of about 463 mm per annum (using a value of 1.53 for the term in square brackets in equation 4). The actual overestimate of  $E_p$  shown in Figure 2 for Mount Gambier is somewhat smaller (380 mm per annum), due to a compensating error in LW irradiance, which is related to underestimated cloudiness in the GCM (discussed below).

[14] These results suggest that the GCM does not adequately resolve cloud systems over southern Australia, consistent with the findings of an earlier model intercomparison based on frontal systems in the Australian midlatitudes [Ryan *et al.*, 2000]. We confirmed this by comparison of the modeled annual-mean cloud cover with satellite-retrieved cloud cover from the International Satellite Cloud Climatology Project (ISCCP) D2 product [Rossow *et al.*, 1996], which indicated a large underestimate by the GCM over southern Australia (not shown). It is worth noting that the resulting errors in modeled  $E_p$  over southern Australia are larger than the observed changes over the last few decades.

#### 4. Conclusions

[15] We have described a simple pan-evaporation model (PenPan), with the radiative component based mostly on work by Linacre [1994], and the aerodynamic component based mostly on work by Thom *et al.* [1981]. PenPan was found to perform well over Australia when forced with observations, which is encouraging, especially as the wind function from Thom *et al.* [1981] was derived under conditions quite different from those in Australia. When forced by output from the CSIRO Mk3 GCM, an overestimate of pan evaporation over southern Australia was primarily due to excessive surface solar irradiance simulated by the GCM. It will be interesting to evaluate the performance of PenPan in other regions, and when forced by other climate models. The results suggest that PenPan will be a valuable tool for the analysis of climate-change simulations, with the aim of understanding and attributing the causes of observed changes in pan evaporation. An attraction of evaporation pans is that they behave approximately as “net radiometers” [Thom *et al.*, 1981], yet the global network of pans is far more extensive than the network of radiometers. Possible improvements to PenPan would be (1) to account for the annual cycle in the calculation of the SW irradiance of the pan (together with a more general treatment of the albedos of the pan and the ground), and (2) to implement a

more accurate treatment of the pan’s LW irradiance (including an allowance for the lower emissivity of the sides of the pan relative to that of the water surface).

[16] **Acknowledgments.** We thank Edward Linacre for helpful discussions and the Australian Bureau of Meteorology for providing the observations. We acknowledge funding support from the Australian Greenhouse Office (LDR), the Managing Climate Variability Program (MLR and GDF), Land and Water Australia Research and Development Corporation (MLR and GDF) and the Gary Comer Award (GDF).

#### References

- Folland, C. K., et al. (2001), Observed climate variability and change, in *Climate Change 2001: The Scientific Basis. Contribution of Working Group I to the Third Assessment Report of the Intergovernmental Panel on Climate Change (IPCC)*, edited by J. T. Houghton et al., pp. 99–181, Cambridge Univ. Press, New York.
- Gordon, H. B., et al. (2002), The CSIRO Mk3 Climate System Model, *Tech. Pap. 60*, 134 pp., CSIRO Atmos. Res., Aspendale, Victoria, Australia. (Available at [http://www.cmar.csiro.au/e-print/open/gordon\\_2002a.pdf](http://www.cmar.csiro.au/e-print/open/gordon_2002a.pdf)).
- Jacobs, A. F. G., B. G. Heusinkveld, and D. C. Lucassen (1998), Temperature variation in a class A evaporation pan, *J. Hydrol.*, *206*, 75–83.
- Kohler, M. A., T. J. Nordenson, and W. E. Fox (1955), Evaporation from pans and lakes, *Res. Pap. 38*, 19 pp., U. S. Dep. of Comm., Washington, D. C.
- Liepert, B. G., J. Feichter, U. Lohmann, and E. Roeckner (2004), Can aerosols spin down the water cycle in a warmer and moister world?, *Geophys. Res. Lett.*, *31*, L06207, doi:10.1029/2003GL019060.
- Linacre, E. T. (1992), *Climate Data and Resources*, 384 pp., Routledge, Boca Raton, Fla.
- Linacre, E. T. (1994), Estimating U.S. Class A pan evaporation from few climate data, *Water Int.*, *19*, 5–14.
- Molina, J. M., V. Martínez, M. M. González-Real, and A. Baille (2006), A simulation model for predicting hourly pan evaporation from meteorological data, *J. Hydrol.*, *318*, 250–261.
- Nazarenko, L., and S. Menon (2005), Varying trends in surface energy fluxes and associated climate between 1960–2002 based on transient climate simulations, *Geophys. Res. Lett.*, *32*, L22704, doi:10.1029/2005GL024089.
- Penman, H. L. (1948), Natural evaporation from open water, bare soil and grass, *Proc. R. Soc., Ser. A*, *193*, 120–145.
- Peterson, T. C., V. S. Golubev, and P. Y. Groisman (1995), Evaporation losing its strength, *Nature*, *377*, 687–688.
- Roderick, M. L. (1999), Estimating the diffuse component from daily and monthly measurements of global radiation, *Agric. For. Meteorol.*, *95*, 169–185.
- Roderick, M. L., and G. D. Farquhar (2002), The cause of decreased pan evaporation over the past 50 years, *Science*, *298*, 1410–1411.
- Roderick, M. L., and G. D. Farquhar (2004), Changes in Australian pan evaporation from 1970 to 2002, *Int. J. Climatol.*, *24*, 1077–1090.
- Roderick, M. L., and G. D. Farquhar (2005), Changes in New Zealand pan evaporation since the 1970s, *Int. J. Climatol.*, *25*, 2031–2039.
- Rossow, W. B., A. W. Walker, D. E. Beusichel, and M. D. Roiter (1996), International satellite cloud climatology project (ISCCP) documentation of new cloud datasets, *WMO/TD 737*, 115 pp., World Meteorol. Org., Geneva.
- Ryan, B. F., et al. (2000), Simulation of a cold front by cloud-resolving, limited-area and large-scale models and model evaluation using in-situ and satellite observations, *Mon. Weather Rev.*, *128*, 3218–3235.
- Stanhill, G., and S. Cohen (2001), Global dimming: A review of the evidence for a widespread and significant reduction in global radiation with discussion of its probable causes and possible agricultural consequences, *Agric. For. Meteorol.*, *107*, 255–278.
- Thom, A. S., J. L. Thony, and M. Vauclin (1981), On the proper employment of evaporation pans and atmometers in estimating potential transpiration, *Q. J. R. Meteorol. Soc.*, *107*, 711–736.
- van Dijk, M. H. (1985), Reduction in evaporation due to the bird screen used in the Australian Class A pan evaporation network, *Aust. Meteorol. Mag.*, *33*, 181–183.

G. D. Farquhar and M. L. Roderick, CRC for Greenhouse Accounting, Research School of Biological Sciences, Australian National University, GPO Box 475, Canberra, ACT 2601, Australia.

L. D. Rotstayn, Marine and Atmospheric Research, Commonwealth Scientific and Industrial Research Organisation, Private Bag 1, Aspendale, Victoria 3195, Australia. (leon.rotstayn@csiro.au)